

International Journal of Modern Physics E
© World Scientific Publishing Company

ISOSPIN DIFFUSION IN ^{58}Ni -INDUCED REACTIONS AT INTERMEDIATE ENERGIES

E. GALICHET*, M. F. RIVET, B. BORDERIE

*Institut de Physique Nucléaire, IN2P3/CNRS, Université Paris-Sud-11, F-91406 Orsay, France
rivet@ipno.in2p3.fr*

M. COLONNA

Laboratori Nazionali del Sud, I-95123 Catania, Italy

R. BOUGAULT, D. DURAND, N. LE NEINDRE, O. LOPEZ, L. MANDUCI, E. VIENT

LPC, ENSICAEN et Université, IN2P3/CNRS, F-14050 Caen, France

A. CHBIHI, J. D. FRANKLAND, J. P. WIELECZKO

GANIL, CEA et IN2P3/CNRS, F-14076 Caen, France

R. DAYRAS, C. VOLANT

IRFU/SPhN, CEA Saclay, F-91191, Gif-sur-Yvette, France

D. C. R. GUINET, P. LAUTESSE

IPN et Université Claude Bernard LyonI, IN2P3/CNRS, F-69622 Villeurbanne, France

M. PARLOG

NIPNE, RO-76900 Bucharest-Măgurele, Romania

E. ROSATO, M. VIGILANTE

Dipartimento di Scienze Fisiche e Sezione INFN, Università Federico II, I-80126 Napoli, Italy

INDRA Collaboration

Received (received date)

Revised (revised date)

Isospin diffusion is probed as a function of the dissipated energy by studying two systems $^{58}\text{Ni}+^{58}\text{Ni}$ and $^{58}\text{Ni}+^{197}\text{Au}$, over the incident energy range 52-74 A MeV. Experimental data are compared with the results of a microscopic transport model with two different parameterizations of the symmetry energy term. A better overall agreement between data and simulations is obtained when using a symmetry term with a potential part linearly increasing with nuclear density. The isospin equilibration time at 52 A MeV is estimated to 130 ± 10 fm/c.

*and Conservatoire National des Arts et Métiers, F-75141 Paris, France

2 *E. Galichet et al.*

1. Introduction

Collisions between nuclei with different charge asymmetries may carry important information on the structure of the nuclear equation of state (EOS) symmetry term in density and temperature regions away from the normal value, that may be encountered along the reaction path. For instance, the symmetry energy behaviour influences reaction processes, such as fragmentation, pre-equilibrium emission, N/Z equilibration between the two collisional partners.^{1,2} Among the sensitive observables, in semi-peripheral collisions, one can study isospin diffusion, either through isospin transport ratios^{3,4} or by using the isotopic content of light particle and IMF emission and the asymmetry (N/Z) of the reconstructed quasi-projectiles (QP) and quasi-targets (QT).^{5,6,7} The degree of equilibration, that is related to the interplay between the reaction time and the typical time for isospin transport, can give information about important transport properties, such as drift and diffusion coefficients, and their relation with the density dependence of the symmetry energy.

We have performed this kind of investigations by studying isospin transport effects on the reaction dynamics for two systems, with the same projectile, ^{58}Ni , and two different targets, ^{58}Ni and ^{197}Au , at incident energies of 52A MeV and 74A MeV.^{6,7} The N/Z ratio of the two composite systems is N/Z=1.07 for Ni+Ni and N/Z=1.38 for Ni+Au. This choice gives access to isospin effects in different conditions of charge (and mass) asymmetry and to *their evolution with the energy deposited into the system*. In the symmetric Ni + Ni system isospin effects are essentially due to the pre-equilibrium emission. On the contrary, in the charge (and mass) asymmetric reactions, one can observe isospin transport between the two partners. The dependence of these mechanisms on the symmetry energy behaviour is discussed.

2. Experiment

2.1. *Experimental details*

^{58}Ni ($179 \mu\text{g}/\text{cm}^2$) and ^{197}Au ($200 \mu\text{g}/\text{cm}^2$) targets were bombarded with ^{58}Ni projectiles accelerated to 52 and 74A MeV by the GANIL facility. The charged products emitted in collisions were collected by the 4π detection array INDRA.⁸ All elements were identified within one charge unit up to the projectile charge. Moreover H to Be isotopes were separated when their energy was high enough (above 3, 6, 8 MeV for p, d, t; 20-25 MeV for He isotopes; ~ 60 MeV for Li and ~ 80 MeV for Be). In the following we shall call fragments the products for which only the atomic number is measured ($Z \geq 5$). As the on-line trigger required four fired modules of the array, the off-line analysis only considered events in which four charged products were identified.⁶

2.2. Event selection

After eliminating events in which less than 90% of the charge of the projectile was detected, we build subevents containing the ensemble of charged products which have a velocity higher than half the laboratory projectile velocity (i.e. forward emitted in the nucleon-nucleon (NN) frame). We call this ensemble “quasi-projectile” (QP) without prejudice on the equilibration of any degree of freedom of the system so defined. This choice eliminates the detection biases on the quasi-target (QT) side and avoids considering products coming from the QT. Finally to get homogeneous samples we ask that the total charge of the QP is comprised between 24 and 32. In all cases 1.3 to 2×10^6 events are kept, amounting to 14-18% of the reaction cross sections.⁶

2.3. The sorting variable

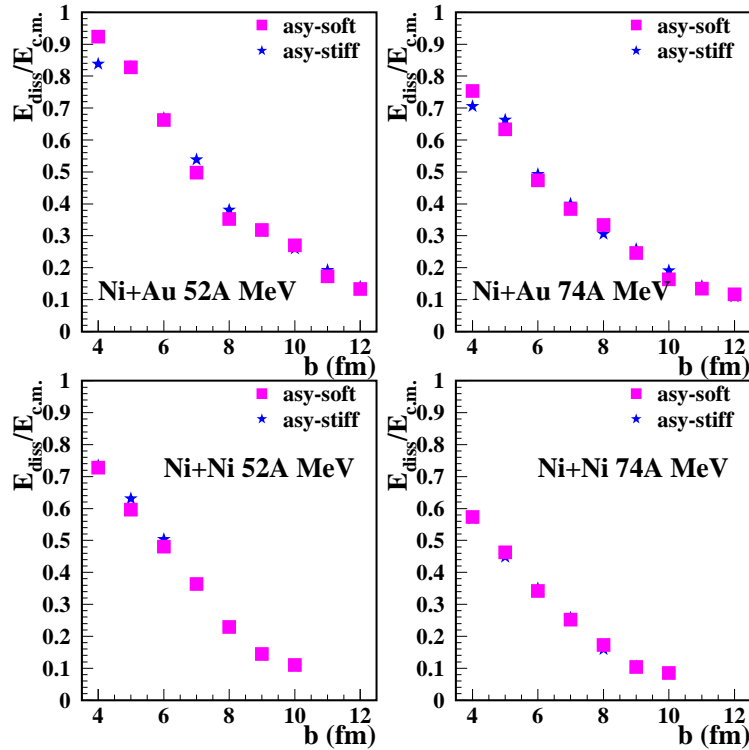


Fig. 1. Correlation between $E_{\text{diss}}/E_{\text{c.m.}}$ and the impact parameter for the four studied systems and two asy-EOS. From.⁷

To follow the isospin diffusion as a function of the violence of the collision, we chose to sort the events as a function of the dissipated energy, calculated in a binary

4 *E. Galichet et al.*

hypothesis without mass transfer:

$$E_{\text{diss}} = E_{\text{c.m.}} - \frac{1}{2}\mu V_{\text{rel}}^2, \quad (1)$$

with μ the initial reduced mass, $E_{\text{c.m.}}$ the available energy and

$$V_{\text{rel}} = V_{\text{QP}}^{\text{rec}} \times \frac{A_{\text{tot}}}{A_{\text{target}}} \quad (2)$$

$V_{\text{QP}}^{\text{rec}}$ is the QP velocity, reconstructed from the velocity of all the fragments it contains. Most of the QP events have only one fragment. For the Ni+Ni system, about 25-30% of the events have two or more fragments while for the Ni+Au system this percentage is smaller ($\sim 15\%$). It is demonstrated in ^{9,10} that the velocity of the QP is a good parameter for following dissipation. The dissipated energy was calculated following the same procedure in the BNV simulations (see next section), and it is shown in fig 1 that there is a close correlation between $E_{\text{diss}}/E_{\text{c.m.}}$ and the impact parameter. A complete description of the experimental findings can be found in. ⁶

3. The BNV transport model

We follow the reaction dynamics solving the BNV transport equation, that describes the evolution of the one-body distribution function according to the nuclear mean-field and including the effects of two-body collisions. The test-particle prescription is adopted, using the TWINGO code ¹¹ with 50 test particles per nucleon. The main ingredients that enter this equation are the nuclear matter compressibility, the symmetry energy term and its density dependence and the nucleon-nucleon cross section. We take a soft isoscalar equation of state, with a compressibility modulus $K = 200$ MeV, which is favoured e.g. from flow studies or from the confrontation data-dynamical simulations at intermediate energies. ^{12,13}

Two different prescriptions for the behaviour of the symmetry energy are used to study the sensitivity of the results to the considered parameterization. Indeed one can write the symmetry energy part of the EOS as the sum of a kinetic term and a potential term (to be multiplied by $[(N - Z)/A]^2$), often approximated, for the sake of comparison, as:

$$\frac{E_{\text{sym}}}{A}(\rho) = \frac{C_{s,k}}{2} \left(\frac{\rho}{\rho_0}\right)^{2/3} + \frac{C_{s,p}}{2} \left(\frac{\rho}{\rho_0}\right)^\gamma \quad (3)$$

where ρ_0 is the nuclear saturation density. The value of the γ exponent, valid close to ρ_0 , determines whether the equation is “asy-stiff” ($\gamma \geq 1$, potential term continuously increasing with ρ) or “asy-soft” ($\gamma < 1$, potential term presenting a maximum between ρ_0 and $2\rho_0$). In this paper we chose as asy-stiff a potential symmetry term linearly increasing with nuclear density ($\gamma=1$), and as asy-soft the *SKM** parameterization in which the potential symmetry term can be approximated with $\gamma=0.5$. ¹⁴

The free nucleon-nucleon cross section with its angular, energy and isospin dependence was used. Indeed, as there is no consistency between the mean field and the residual interaction in transport codes, there is no reason to adopt an in-medium correction which may be “valid” with one specific mean field. For instance good reproductions of nuclear dynamics above $40A$ MeV were obtained using the free nucleon-nucleon cross section. ^{15,16}

For the two reactions, we have ran different impact parameters, from $b=4$ fm to $b=10$ fm for the Ni+Ni system and from $b=4$ fm to $b=12$ fm for the Ni+Au system. For each impact parameter 10 events were produced (one event represents already the mean trajectory of the reaction), for the two cases of symmetry energy parameterization. The detailed analysis of the results of the simulations can be found in. ⁷

4. Isospin diffusion

The measure of isospin diffusion ideally requires the determination of the ratio N/Z for hot quasi-projectiles, just after QP and QT separate. Experimentally it is however not possible to fully reconstruct the primary QP because neutrons are not measured and the masses of the heavier fragments are not known. We chose to construct an isospin-dependent variable from the isotopically identified particles included in the QP:

$$(\langle N \rangle / \langle Z \rangle)_{\text{CP}} = \sum_{N_{\text{evts}}} \sum_{\nu} N_{\nu} / \sum_{N_{\text{evts}}} \sum_{\nu} P_{\nu} \quad (4)$$

where N_{ν} and P_{ν} are respectively the numbers of neutrons and protons bound in particle ν , ν being d, t, ^3He , ^4He , ^6He , ^6Li , ^7Li , ^8Li , ^9Li , ^7Be , ^9Be , ^{10}Be ; free protons are excluded. N_{evts} is the number of events contained in the dissipated energy bin considered. The variable $(N/Z)_{\text{CP}}$ was calculated twice: first considering particles forward emitted in the nucleon-nucleon frame ($V_{\text{particle}} > V_{\text{proj}}^{\text{lab}}/2$), and secondly keeping only particles forward emitted in the QP frame ($V_{\text{particle}} > V_{\text{QP}}^{\text{rec}}$). Indeed as the BNV simulation does not allow to identify mid-rapidity particles and light fragments, the theoretical value of $(N/Z)_{\text{CP}}$ is calculated only from the particles evaporated by the QP, which we experimentally approximate as the particles forward emitted in the QP frame.

4.1. Isospin diffusion in BNV simulations

The evolution of the N/Z ratio of the quasi-projectiles as a function of $E_{\text{diss}}/E_{\text{c.m.}}$ is reported in fig. 2. $(N/Z)_{\text{QP}}$ increases with the centrality of the collision for the two systems and the two beam energies. For the Ni+Ni system the variation of $(N/Z)_{\text{QP}}$ with centrality is small, and attributed to pre-equilibrium emission. Little dependence on the EOS appears at $52 A$ MeV, while $(N/Z)_{\text{QP}}$ grows slightly higher at $74 A$ MeV for the asy-stiff case. Indeed, for this system with a small neutron excess, more protons are emitted during the pre-equilibrium stage due to the coupled

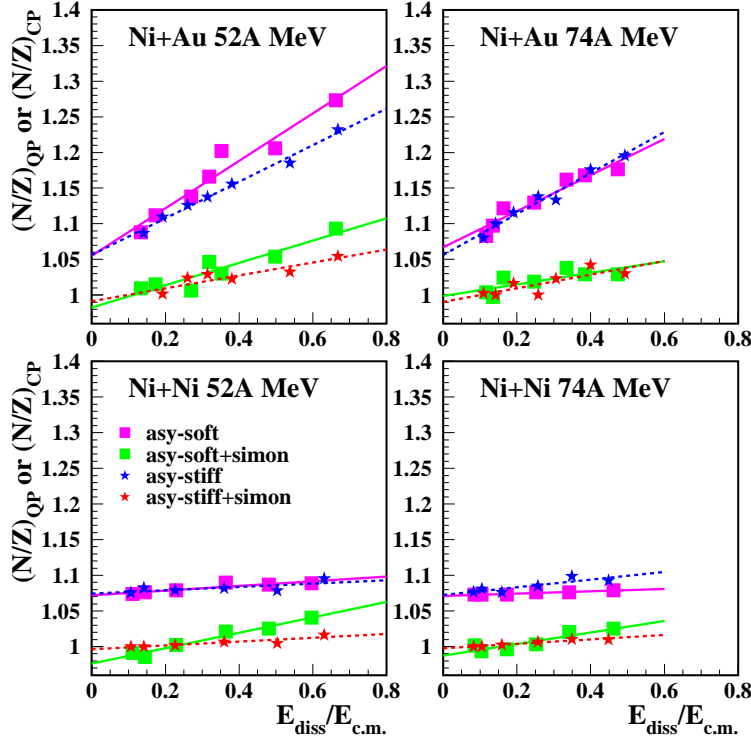
6 *E. Galichet et al.*


Fig. 2. Upper curves in each panel: isospin ratio of hot QP, $(N/Z)_{QP}$, vs $E_{diss}/E_{c.m.}$ obtained in the simulation with two asy-EOS (blue stars for asy-stiff and pink squares for asy-soft). The evolution of the variable $(N/Z)_{CP}$ obtained after de-exciting the QP with SIMON is represented by the lower curves (red stars and green squares). The lines correspond to linear fits. Adapted from.⁷

effect of Coulomb repulsion and a less attractive symmetry potential for protons. This effect increases with the incident energy. On the contrary, the asy-soft case tends to emit more pre-equilibrium neutrons leading to a lower N/Z ratio.¹⁷

The evolution with centrality is much more pronounced for the neutron-rich and asymmetric Ni+Au system. In addition to pre-equilibrium effects, isospin transport takes place between the two partners of the collision, and increases with the violence of the collision. $(N/Z)_{QP}$ is mostly higher in the asy-soft than in the asy-stiff case for the two energies. The largest value reached, corresponding to $b=4$ fm, is lower at 74 A MeV than at 52 A MeV; this may be attributed to the shorter reaction times, and to the fact that the collision becomes more transparent. Thus the N/Z diffusion appears related to the degree of dissipation reached in the system and to the driving force provided by the symmetry term of the nuclear EOS, that speeds up the isospin equilibration among the reaction partners. An asy-soft EOS, more dissipative, favours isospin equilibration between the two partners, as found also in

other recent theoretical investigations. 18,3,1,19,20

4.2. *Effects of secondary decay*

In figure 2 are also plotted the results concerning the variable $(N/Z)_{\text{CP}}$, calculated after de-exciting the hot primary QPs with the help of the SIMON code.²¹ The values of $(N/Z)_{\text{CP}}$ are always smaller and the evolution with dissipation is generally flatter than that of the N/Z of the primary QP: *secondary decay weakens the isospin effects.*

At 52 A MeV however the differences between the results of the two parameterizations are more pronounced for $(N/Z)_{\text{CP}}$, with respect to $(N/Z)_{\text{QP}}$. Indeed excitation energies are larger in the asy-soft case, which favours the emission of neutron-richer particles, and thus enhances the effect due to the larger N/Z value observed in that case for the QP. At 74 A MeV, no discrimination between the asy-EOS is possible for Ni+Au (as was already the case for hot QPs), whereas for the reaction Ni+Ni the effects due to the de-excitation modify the initial trend imposed by the dynamical evolution: the values of $(N/Z)_{\text{QP}}$ are larger in the asy-stiff case; conversely the associated $(N/Z)_{\text{CP}}$ are smaller than those obtained in the asy-soft case.

Finally $(N/Z)_{\text{CP}}$, which appears in the simulations to be linearly correlated with the N/Z of the primary QP, is a good indicator of isospin transport effects and is sensitive to the asy-EOS.

4.3. *Comparison between experimental and simulated data*

The evolution of the experimental values of $(N/Z)_{\text{CP}}$ with dissipation is displayed in fig 3. Open points show the values obtained forward in the NN frame. Let us remind that in this case we mix mid-rapidity particles and those coming from the QP de-excitation. For the Ni+Ni system at both incident energies, $(N/Z)_{\text{CP}}$ varies by at most 1.5% when dissipation increases. This is the expected behaviour for this symmetric system where N/Z is only modified by pre-equilibrium emission, as explained in the previous subsection. For the Ni+Au system the isospin ratio is higher than that of the Ni+Ni system whatever the dissipated energy. For the three first bins of dissipated energy $(N/Z)_{\text{CP}}$ has the same value for the two incident energies and slightly decreases with dissipation; this is due to the on-line trigger.⁶ The isospin ratio of the Ni+Au system is however higher than that of the Ni+Ni system, which could arise from the neutron skin of the Au target and/or from the mid-rapidity particles included in our quasi-projectile selection which are more neutron rich.^{22,23} This result is a first indication of isospin diffusion. At higher dissipated energies, $(N/Z)_{\text{CP}}$ presents a significant increase with dissipation and reaches higher values at 52A MeV, while the trend is flatter at 74A MeV. This may be interpreted as a progressive isospin diffusion when collisions become more central, in connection with a larger overlap of the reaction partners and thus a longer

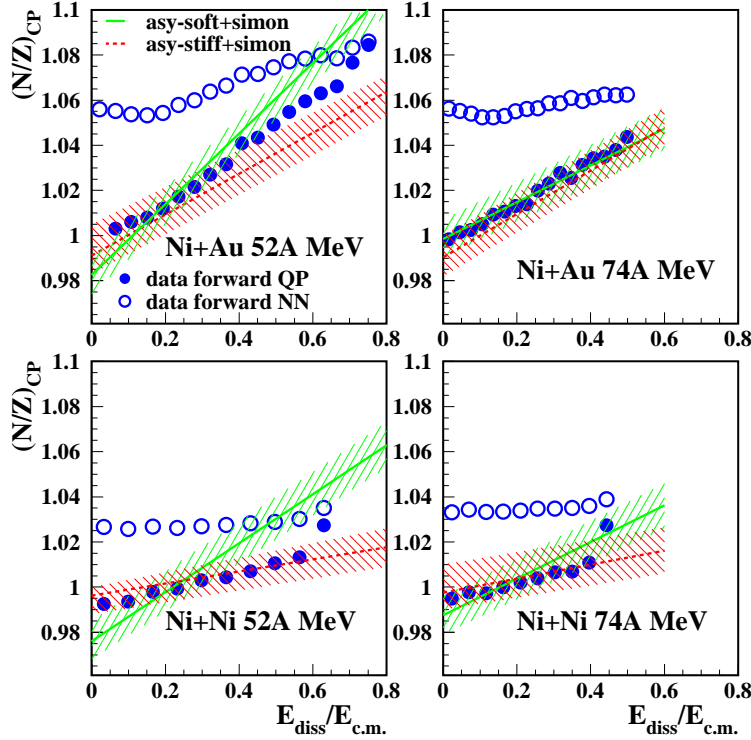


Fig. 3. Isospin ratio of complex particles, $(N/Z)_{CP}$, vs $E_{diss}/E_{c.m.}$. Circles correspond to experimental data: open, forward in NN frame, close, forward in QP frame. Error bars are within the size of the symbols. Dotted and solid lines are as in fig 2 and hatched zones give error bars from simulations. Adapted from. ⁷

interaction time. For a given centrality, the separation time is longer at 52A MeV than at 74A MeV, leaving more time to the two main partners to go towards isospin equilibration.

The close points in fig 3 are related to the values of $(N/Z)_{CP}$ forward in the QP frame. They are in all cases smaller than the previous ones, and for Ni+Au at both energies, they grow faster with dissipation. This is because the mid-rapidity particles are no longer included: it is known that these particles are more neutron-rich, and that their isospin content is independent of the violence of the collision. ²² The values of $(N/Z)_{CP}$ forward in the QP frame are compared with the results of the simulation, displayed in fig 3 by the lines and the hatched zones. A first result worth mentioning is that the chemical composition (N/Z) of the quasi-projectile forward emission appears as a very good representation of the composition of the entire quasi-projectile source. Such an observation seems to validate a posteriori the selection frequently used to characterize the QP de-excitation properties.

When looking *globally* at the results for the four cases treated here, the agree-

ment is better when the asy-stiff EOS is used, i.e. a linear increase of the potential term of the symmetry energy around normal density. Note however that for Ni+Au at 52 A MeV, where isospin transport effects are dominant, the close points lie in between the simulated results with the two EOS. This observation allows us to put an error bar on our result, expressed as $\gamma=1\pm 0.2$ (see Eq. (3)). This value is in reasonable agreement with that recently obtained from isospin diffusion in Sn+Sn systems at 50 A MeV⁴, and matches the one derived from the competition between dissipative mechanisms for Ca+Ca,Ti at 25 A MeV.²⁴

5. Isospin equilibration time

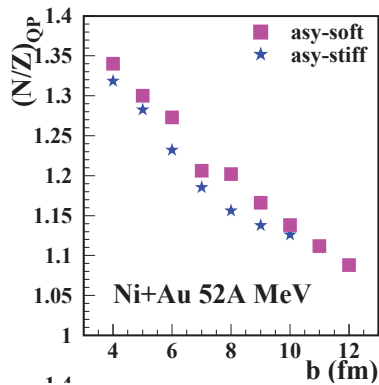


Fig. 4. Isospin ratio of primary Ni QP vs the impact parameter obtained in BNV simulations for the Ni+Au system at 52 A MeV. Adapted from.⁷

The knowledge of the different time scales associated to the various degrees of freedom involved in heavy-ion collisions at intermediate energy is of crucial importance to determine the physical properties of nuclear sources produced in the exit channel. Particularly with the announced exotic beams the N/Z degree of freedom will hopefully be explored over a wide range, and thus an estimate of the chemical (isospin) equilibration time becomes essential. It turns out that we can extract this information from the present data. Fig 4 shows, for the Ni+Au system at 52 A MeV, the evolution of the N/Z of the primary QP with the impact parameter obtained in BNV simulations. The equilibrium value, $N/Z=1.38$, is almost reached for $b=4$ fm, at the time when the QP and QT separate. This time is equal to 130 ± 10 fm/c. A similar value of 115 fm/c has been reported for the Zn+Au system at 47 A MeV.²⁵ Interestingly enough the equilibration of isospin can be derived directly from the experimental data. In the top-left panel of fig 3 one observes that the open and close points superimpose at high dissipation: the values of $(N/Z)_{CP}$ are the same at mid-rapidity and at velocities close to that of the QP. This is a strong indication of isospin equilibration. Note that more than 75% of the energy must have been dissipated before equilibrium is reached. Qualitatively this high value of the dissipated energy at isospin equilibration pleads for an asy-stiff EOS, as was shown

when considering isospin transport ratios in simulated Sn+Sn collisions at 35 and 50 A MeV. ²⁰

6. Conclusions

We studied isospin transport as a function of dissipation or centrality in heavy-ion collisions for two beam energies, looking directly at the average isotopic content of the light particles emitted by the quasi-projectile.

Experimentally we followed an isospin-dependent variable, $(N/Z)_{CP}$, constructed with the identified isotopes belonging to quasi-projectiles, as a function of the dissipated energy. Its value very slightly increases with centrality for the Ni+Ni system, for which no isospin transport effect is expected, whereas it evolves much more for Ni+Au, indicating the presence of isospin transport.

Simulations show that for the Ni + Ni system, the N/Z of the quasi-projectile is essentially determined by proton rich pre-equilibrium emission, and thus slightly increases with centrality. The effect is more pronounced using an asy-stiff equation of state. For the Ni+Au system isospin transport takes place and the N/Z is larger in the asy-soft case. After de-excitation of the hot QPs, the isospin effects, although weaker, are still present and the variable $(N/Z)_{CP}$ is sensitive to the asy-EOS. The non-negligible effect of evaporation necessitates a precise knowledge of the evaporation properties of medium-mass exotic nuclei; the INDRA Collaboration has initiated an experimental program in that aim.

The results of the simulations are analysed in the same way as the experimental data. This demonstrates that $(N/Z)_{CP}$ is linearly related to $(N/Z)_{QP}$. When considering the four cases under study we find a better overall agreement between simulations and experimental data for the asy-stiff case corresponding to a potential symmetry term linearly increasing with nuclear density. Referring to Eq. (3) we propose a value $\gamma=1\pm 0.2$. Information concerning the isospin equilibration time, is also obtained. At 52 A MeV for the Ni+Au and the most dissipative collisions we can infer from the data-model comparison that isospin equilibration is reached at 130 ± 10 fm/c.

References

1. V. Baran, M. Colonna et al., *Phys. Rep.* **410** (2005) 335.
2. Bao-An Li, Lie-Wen Chen and Che Ming Ko, *Phys. Rep.* **464** (2008) 113.
3. M. B. Tsang, T. X. Liu et al., *Phys. Rev. Lett.* **92** (2004) 062701.
4. M. B. Tsang, Y. Zhang et al., *Phys. Rev. Lett.* **102** (2009) 122701.
5. D. V. Shetty, S. J. Yennello et al., *Phys. Rev.* **C 70** (2004) 011601.
6. E. Galichet, M. F. Rivet et al. (INDRA Collaboration), *Phys. Rev.* **C 79** (2009) 064614.
7. E. Galichet, M. Colonna et al., *Phys. Rev.* **C 79** (2009) 064615.
8. J. Pouthas, B. Borderie et al., *Nucl. Instr. and Meth. in Phys. Res.* **A 357** (1995) 418.
9. R. Yanez, S. Hudan et al., *Phys. Rev* **C 68** (2003) 011602.

10. S. Piantelli, P. R. Maurenzig et al., *Phys. Rev. C* **74** (2006) 034609.
11. A. Guarnera, M. Colonna and P. Chomaz, *Phys. Lett. B* **373** (1996) 267.
12. P. Danielewicz, R. Lacey and W. G. Lynch, *Science* **298** (2002) 1592.
13. B. Borderie and M. F. Rivet, *Prog. Part. Nucl. Phys.* **61** (2008) 551.
14. V. Baran, M. Colonna et al., *Nucl. Phys. A* **703** (2002) 603.
15. F. Haddad, B. Borderie et al., *Z. Phys. A - Hadrons and Nuclei* **354** (1996) 321.
16. E. Galichet, F. Gulminelli et al. (INDRA Collaboration), *Eur. Phys. J. A* **18** (2003) 75.
17. R. Lioni, V. Baran et al., *Phys. Lett. B* **625** (2005) 33.
18. L. Shi and P. Danielewicz, *Phys. Rev. C* **68** (2003) 064604.
19. L. W. Chen, C. M. Ko and B. A. Li, *Phys. Rev. Lett.* **94** (2005) 032701.
20. J. Rizzo, M. Colonna et al., *Nucl. Phys. A* **806** (2008) 79.
21. D. Durand, *Nucl. Phys. A* **541** (1992) 266.
22. T. Lefort, D. Doré et al. (INDRA Collaboration), *Nucl. Phys. A* **662** (2000) 397.
23. E. Plagnol, J. Lukasik et al. (INDRA Collaboration), *Phys. Rev. C* **61** (1999) 014606.
24. F. Amorini, G. Cardella et al., *Phys. Rev. Lett.* **102** (2009) 112701.
25. S. Kowalski, J. B. Natowitz et al., *Phys. Rev. C* **75** (2007) 014601.